Biotechnology and Bioprocess Engineering 17: 746-754 (2012)
DOI 10.1007/s12257-012-0046-x

RESEARCH PAPER

Surface Reactivity and *in vitro* Biological Evaluation of Sol Gel Derived Silver/calcium Silicophosphate Bioactive Glass

Nader Nezafati, Fathollah Moztarzadeh, and Saeed Hesaraki

Received: 23 January 2012 / Revised: 2 April 2012 / Accepted: 3 April 2012

Abstract Ag ions are known for their antibacterial effects. Ag containing silicate glasses have been extended to create bioactive glasses that exhibit inhibitory effects on bacterial growth using different techniques. In this work, calcium and calcium/silver silicophosphate glasses were synthesized from the sol-gel process and their physico-chemical and *in vitro* biological properties were studied and compared. The effect of silver concentration on *in vitro* bioactivity and antibacterial properties of the glasses was investigated. Ag_2O was substituted for CaO in the glass formula up to 2 mol% and *in vitro* bioactivity of the samples was evaluated by soaking them in simulated body fluid followed by structural characterization using XRD, FTIR and SEM techniques. The results showed that both glasses favored precipitation of the calcium phosphate layer when they were soaked in simulated body fluid; however, the morphology of apatite crystals changed for the 2% mol silver containing sample. Substitution of 2% mol Ag_2O for CaO seemed to slightly stimulate the rate of precipitation. The in vitro biodegradation rate of the silver/calcium silicophosphate glasses was lower than that of the silver-free one (control). Also, the antibacterial properties of the samples indicated that these effects were improved by increasing silver concentration in bioactive glass composition.

Keywords: silver, apatite crystals, biodegradation rate, antibacterial properties

Nader Nezafati, Fathollah Moztarzadeh*
Biomaterials Group, Faculty of Biomedical Engineering (Center of Excellence), Amirkabir University of Technology, Tehran, Iran
Tel: +98-21-6454-2393; Fax: +98-21-6646-8186
E-mail: moztarzadeh@aut.ac.ir

Saeed Hesaraki
Nanotechnology and Advanced Materials Department, Materials and Energy Research Center, Karaj, Iran

1. Introduction

Bioactive glasses are an important group of materials with a wide range of applications in medicine as bone substitutes. These materials are able to bind with bones in a living organism through forming a layer of hydroxyapatite (HA) on their surfaces [1]. Bioactive glasses can be obtained by melting a dried batch of starting materials at elevated temperatures or by a low temperature process known sol-gel [2]. The sol-gel method has several advantages such as high purity, ultrahomogeneity, low processing temperatures, and most significantly the possibility of making glasses of new compositions [3].

Many researchers have focused on the preparation and characterization of bioceramic-based biomaterials, whether crystalline bioceramics or amorphous bioglasses, incorporated with ions such as Zn, Mg, and Si due to their unique effect on osteoblastic cell proliferation, differentiation and thus bone mineralization [4-7].

Many researchers have preferred studying sol–gel derived bioactive glasses containing SiO_2, CaO and P_2O_5 as the main components of glass composition [8-10]. The presence of SiO_2 in the composition of bioactive glasses is important because of its function as a network former in the glass structure. In addition, Si–OH groups produced from the exchange process of Ca^{2+} ions (from glass) with H_3O^+ (from solution) are susceptible sites for calcium phosphate nucleation [11,12]. Meanwhile, the presence of Si ions released from the glass composition into the cell culture medium can improve cell functions [13,14]. P_2O_5 is also used to aid nucleation of calcium phosphate phase on the glass surfaces [8].

Many approaches have been investigated in order to enhance the bioactivity of bioactive glasses towards the physiological environment by incorporating various metal

ions in the silicate network.

For example, magnesium and zinc ions were separately added to these components to form $CaO–ZnO–SiO_2–P_2O_5$ or $CaO–MgO–SiO_2–P_2O_5$ bioactive glass systems due to their stimulatory effects on cell proliferation and bone formation, and were evaluated in terms of physical, physico-chemical and biological properties [15].

Both metallic and ionic silver were incorporated into several biomaterials such as polyurethane [16], hydroxyapatite [17] and bioactive glasses. The antibacterial activity of silver ions and their biological impact have been reported in many works [18-20].

Although the biological and antibacterial effects of silver ions on the glass structure have been extensively studied [21-27], only few studies have been reported on *in vitro* surface reactivity and physico-chemical interactions of these kinds of bioactive glasses in simulated body fluid (SBF) solution.

The objective of the present study was to produce a sol–gel derived bioactive silicophosphate glass based on $SiO_2–CaO–Ag_2O–P_2O_5$ system with different molar ratios of silver oxide in the glass composition and compared its physicochemical, bioactivity and antibacterial properties to those of a silver-free bioactive glass using proper analytical techniques.

2. Materials and Methods

2.1. Preparation of the Ag-BGs

The starting materials for the synthesis of the Ag-BG and silver-free samples were tetraethylorthosilicate (TEOS: $C_8H_{20}O_4Si$), triethyl phosphate (TEP: $C_6H_{15}O_4P$), calcium nitrate ($Ca(NO_3)_2.4H_2O$), silver nitrate $Ag(NO_3)_2.4H_2O$, ammonia and nitric acid. Using a typical procedure, the samples were prepared by the sol–gel method with different molar ratios of calcium and silver as listed in Table 1. The silver containing bioactive glass is named Ag-BG. In this research, the terms Ag-free BG, silver free bioactive glass and control sample are all used synonymously.

In this regard, TEOS (20 mL) and distilled water (40 mL) together with 2 mol/L HNO_3 (2.8 mL) were dissolved in ethanol (80 mL) and stirred at room temperature for 30 min. TEP (2.2 mL) was then dissolved into the prepared acid silica sol. After stirring for 20 min, calcium nitrate and silver nitrate (if necessary) were added into the acid sol. 1.0 mol/L concentration of ammonia solution (25 mL) was dropped into the acid sol with vigorously stirring after silver nitrate was completely dissolved. Following this, the sol suddenly gelated. The obtained gel was stirred using a magnet in order to avoid the formation of bulk gel. The resulting gel was kept in an oven for 1 day at 70°C to remove the residual water and ethanol. The dried gel powders were heated at 700°C in a furnace at the rate of 5°C/min and maintained at this temperature for 24 h to eliminate organics and form glass particles. The obtained powders were ground in a planetary mill for 1 h. All the abovementioned reagents were received from Merck Company and used without any purification.

Table 1. The chemical composition of prepared samples

Notation	Composition (mol%)			
	SiO_2	CaO	P_2O_5	Ag_2O
Ag free-BG (control)	64	28	8	0
0.5% Ag-BG	64	27.5	8	0.5
1% Ag-BG	64	27	8	1
2% Ag-BG	64	26	8	2

2.2. *In vitro* surface reactivity test

The in vitro surface reactivity of the glasses was conducted on disc-shaped samples (10 mm in diameter and 2 mm in height) formed by pressing the glass powder in a hydraulic press device at 9 MPa followed by heating at 700°C. The samples were then soaked in simulated body fluid (SBF) at solid (S) to liquid (L) loading of 1 g/100 mL and then kept at 37°C for various periods up to 14 days. The SBF solution was prepared according to the procedure described by Kokubo *et al*. [28], by dissolving NaCl 8.035 g/L, KCl 0.225 g/L, $K_2HPO_4·3H_2O$ 0.231 g/L, $MgCl_2·6H_2O$ 0.311 g/L, $CaCl_2$ 0.292 g/L, $NaHCO_3$ 0.355 g/L, and Na_2SO_3 0.072 g/L into distilled water, buffered at pH = 7.25 with 6.118 g/L tris-hydroxymethyl aminomethane and 1 N HCl solution at 37°C. The SBF solution was chosen because of its characteristic of being highly supersaturated characteristic with respect to apatite. The SBF composition compared with human blood plasma where is shown in Table 2. According to Oyane and Takadama [29,30], the SBF solution is so far the best solution for *in vitro* measurement of apatite-forming ability in implant materials.

The phase composition of the synthesized Ag-BG and Ag-free BG samples was studied after incubation for 24 h

Table 2. Ion concentrations of human blood plasma and SBF

Ion	Plasma (mmol/L)	SBF (mmol/L)
Na^+	142.0	142.0
K^+	5.0	5.0
Mg^{+2}	1.5	1.5
Ca^{+2}	2.5	2.5
Cl^-	103.0	147.8
HCO_3^-	27	4.2
HPO_4^{-2}	1.0	1.0
SO_4^{-2}	0.5	0.5

and soaking in the SBF solution for 3, 7, and 14 days. For this purpose, phase analysis of the control and Ag-BG samples was performed by a Philips PW3710 diffractometer. This instrument worked with voltage and current settings of 40 kV and 30 mA, respectively and utilized Cu-Kα radiation (1.54 Å). For qualitative analysis, X-Ray diffraction (XRD) diagrams were recorded in the interval $10^o \leq 2\theta \leq 50^o$ at the scan speed of 2^o/sec.

The surface morphology and microstructure of the Ag-BG and Ag-free BG samples were evaluated using scanning electron microscope (SEM) after soaking in the SBF solution. The Ag-BG samples and BG (control) were coated with a thin layer of Gold (Au) by sputtering (EMITECH K450X, England). The morphology was observed on a SEM-Philips XL30 which operated at the acceleration voltage of 15 kV.

An ion release study was performed by immersion of the samples (with the same surface area) in SBF (with S/L ratio mentioned elsewhere) at 37ºC for different time periods: 3, 7, and 14 days. All the reacted solutions were saved for inductively coupled plasma (ICP-AES; Varian Co., USA) analysis of Si, Ca, P, Ag (for Ag-BG specimens) to measure ionic concentrations in the SBF solutions. The SBF was not renewed during the time periods (static protocol). About fifty ml solution was collected from each test after different soaking times in SBF.

The chemical groups in 2% Ag-BG were examined by Fourier transform infrared (FTIR) analysis after different soaking times in the SBF solution. Fine powders of specimens were mixed with KBr powder in the ratio of 1:100 and transparent homogenous discs were formed by pressing the mixture under 5 ton/cm^2 pressure. In this test, data were collected at room temperature at the wavenumber range of 4,000 ~ 400/cm using a spectrometer Bruker Vector 33.

2.3. Antibacterial test

The antibacterial activity of Ag-BG and Ag-free BG discs against *Escherichia Coli* (ATCC 25922) was tested by the agar disc diffusion test (halo test). *E. coli* is as an example of gram-negative bacteria which has been found in biomaterial-related infection sites and is responsible for more than 80% of all these infections. The antibacterial efficiency was determined using a method in which a 100 μL portion of the diluted inoculation was applied to the LB-agar medium and incubated for 30 min at 37ºC for diffusion of diluted inoculation to the LB-agar medium. The discs of approximately 10 mm in diameter and 2 mm in thickness were then placed in these media and incubated at 37ºC for 24-h. Surfaces were removed from the LB-agar medium at the end of the incubation period and the colonies were photographed. In the agar plate test, the antibacterial property was determined by the ratio (w/d) of the width of antibacterial halo (w) and the diameter of the samples (d). The same test was repeated 4 times for each datum. The pH values of the control and 2% Ag-BG samples were measured after different soaking time of the samples in the medium.

2.4. Statistical analysis

Data were processed using Microsoft Excel 2003 software and the results were presented as mean ± standard deviation of at least 4 experiments. Significance between the mean values was calculated using standard software program (SPSS GmbH, Munich, Germany) and $p \leq 0.05$ was considered significant.

3. Results

3.1. XRD analysis

Fig. 1 shows the XRD patterns of the control group and Ag-BGs samples after 3 days (Fig. 1A), 7 days (Fig. 1B) and 14 days (Fig. 1C) of soaking in the SBF solution. In all

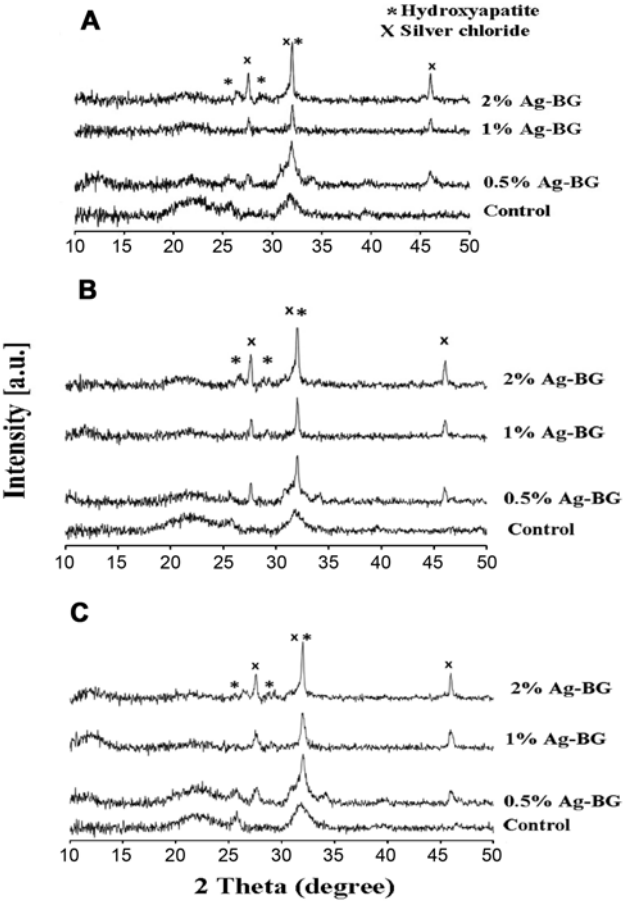

Fig. 1. XRD patterns of Ag-BGs and control samples, (A) after 3 days, (B) 7 days, and (C) 14 days of soaking in SBF.

figures, there were peaks at around 27.6°, 32.05°, and 46.05° which could be related to cubic face-centered AgCl forms corresponding to scattering forms of (111), (200) and (220), respectively (JCPDS Card File No. 31-1238). A peak at around 2θ =32 was also observed which could be attributed to (211) atomic planes of the apatite phase (standard card No JCPD 09-0432). In the samples soaked for 3 days, there was a noticeable peak at about 2θ =32 related to the 2% Ag-BG sample which was sharper than the other samples. This peak for the 1% Ag-BG sample was lower than the 0.5 and 2% Ag-BG samples. The same results were also perceived after 7 and 14 days of soaking time (Figs. 1B and 1C). It should also be noted that all the mentioned peaks of the samples containing silver were sharper than the control sample. As it can be observed in all the figures, the two peaks of silver chloride and the apatite phase were very close to each other (according to the JCPDS). The reason for the formation of these sharp peaks can be due to the overlapping AgCl diffraction and apatite peak. The sharp peak related to the 1% Ag-BG sample was lower than the other silver containing samples (*i.e.:* 0.5 and 2% Ag-BG samples) due to the presence of more considerable silver chloride layer. According to the Figs. 1A, 1B, and 1C, for Ag-BG samples, the intensity of the peak at 2θ =32 became larger by increasing intervals of soaking times. This peak was also found for silver free bioactive glass at all periods of soaking. It should be taken into consideration that the peak width was slightly broadened by increasing the soaking time.

3.2. SEM analyses

Fig. 2 shows the SEM micrographs of the samples after 14 days immersion in the SBF solution. Ball-like particles covered by a layer of entangled rough crystals were observed in these Figures. It is clear from the pictures that the size of the balls and the roughness of the crystals were higher in the 2% silver containing glass (Fig. 2A) than those of the other samples (Figs. 2B, 2C, and 2D). It seems that a certain amount of silver ions stimulated the growth of the calcium phosphate layer.

In addition, high magnification SEM micrographs (Fig. 2E) of the 2% Ag-BG sample showed that apatite crystals with the plate-like nanostructure were oriented perpendicular to the surface of the sample.

The spherical morphology of particles containing plate-like crystals was observed on the surfaces of Ag-BGs. Furthermore, the size and roughness of the crystals of Ag-BGs were higher than the silver free sample.

3.3. ICP measurement

The release behavior of different ions (*i.e.:* silver, silicon and calcium) into the SBF solution was investigated.

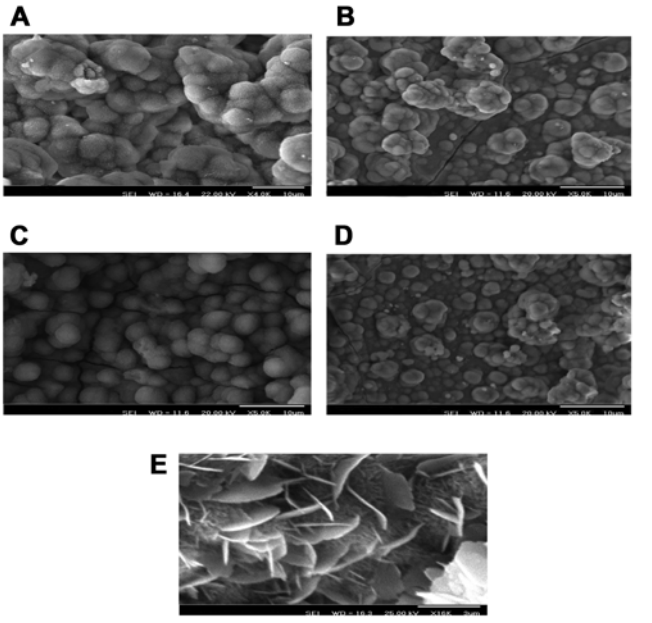

Fig. 2. SEM micrographs of (A) 2% Ag-BG; (B) control samples; (C) 0.5% Ag-BG; (D) 1% Ag-BG; and (E) high magnification SEM micrographs of 2% Ag-BG after immersion for 14 days in SBF solution.

Figs. 3A, 3B, and 3C show the variations in concentrations of Si, Ca and Ag ions in the solution for various periods versus immersion time, respectively. When the Ag-BG samples were reacted with SBF, both chemical and structural changes occured as a function of time. A rapid release of Si was observed from the glass during the first period of immersion which was followed by a decrease in its release rate in other days (Fig. 3A). A rapid increase of Ca concentration occurred during the 2 days for the silver-free and 0.5% silver containing bioactive glasses, during the 4 days for the 2% silver-containing glasses and during the 6 days for the 1% Ag-BG. This was due to a higher rate of dissolution process compared with the precipitation one (Fig. 3B). Dissolution rate of calcium decreased almost after day 3 for the 0.5% silver bioactive glass and control, after day 5 for the 2% silver containing bioactive glass and after day 7 for the 1% Ag-BG probably due to the formation of the apatite layer/AgCl (for especially 1% Ag-BG) onto the surfaces of the specimens; However, it was still more dominant than the precipitation phenomenon. The dissolution of the silver species was relatively slow (Fig. 3C).

3.4. FTIR analysis

Fourier transform infrared spectroscopy (FTIR) is a very useful technique used to examine the structure transformation of materials. Fig. 4 shows FTIR spectra of 2% Ag-BG sintered at 700°C, following immersion in SBF as a function of time.

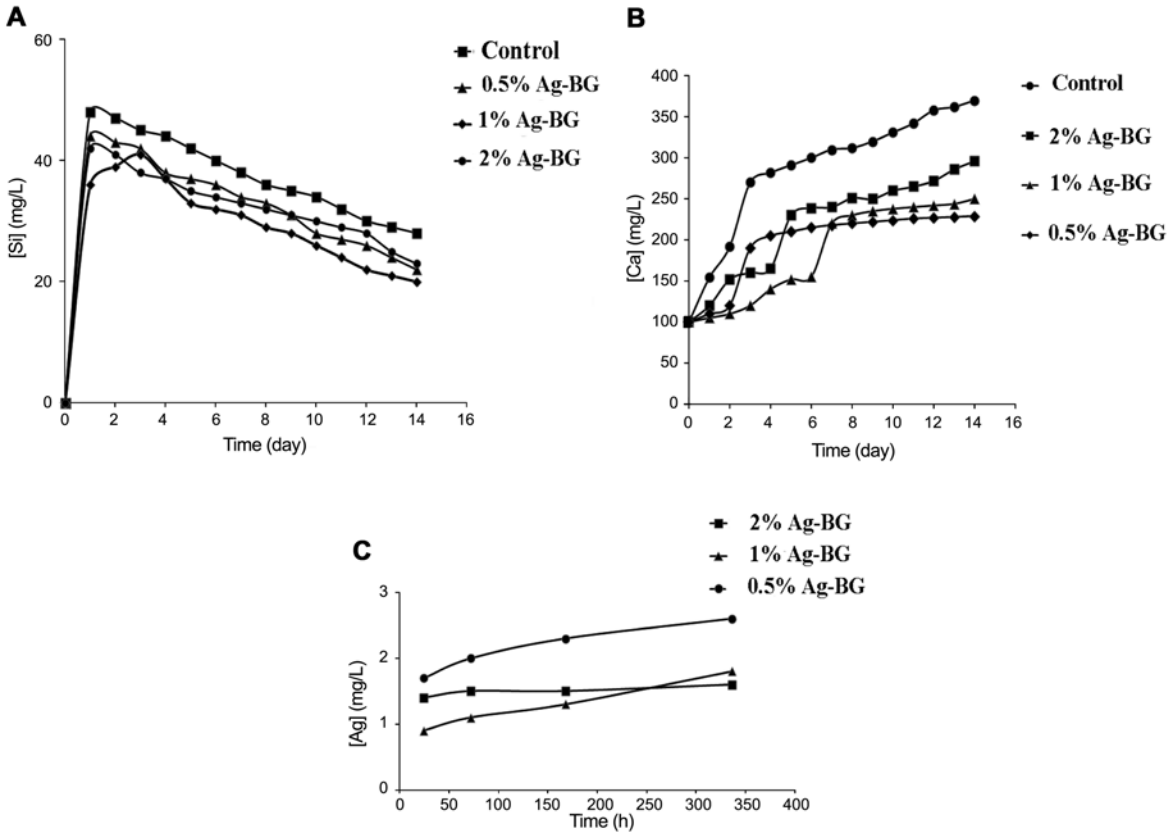

Fig. 3. The variations in concentrations of (A) Si, (B) Ca, and (C) Ag ions in the SBF solution for various periods (measured by ICP-AES) versus immersion time.

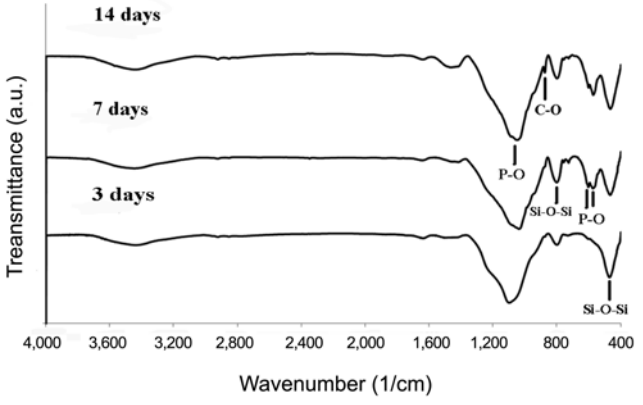

Fig. 4. The FTIR analysis of 2% silver containing sample at different times of soaking in SBF solution.

The diffuse reflectance FTIR spectrum of 2% Ag-BG showed broad bands at about 1,230, 800, and 470/cm corresponding to Si-O-Si stretching, vibrational and bending modes [31,32]. A broad peak at near 1,060/cm indicated P-O bending vibrations in amorphous hydroxyapatite. Peaks at around 604 and 575/cm corresponded to the bending vibrations of P-O bonds of crystalline hydroxyapatite [33-35]. The peak at 876/cm showed vibrational modes of C-O bonds of the carbonate groups in the hydroxyapatite [36]. Therefore, the formation of the hydroxycarbonate apatite (HCA) layer was observed on the surface of 2% Ag-BG after 14 days of soaking. In fact, crystallization of the HCA layer had occurred. With increasing time of immersion in SBF, the intensities of the peaks corresponding to the vibrational modes of P-O increased relative to those relating to Si-O-Si.

3.5. Antibacterial test

Antibacterial properties of the samples with different silver molar ratios are shown in Fig. 5 and Table 3. Fig. 5 shows a picture of the antibacterial ring of the Ag-BG and Ag-free bioglass samples, which indicates the antibacterial property. As shown in Table 3, all samples showed 100% bactericidal ratio and the sample with a molar ratio of 2% Ag exhibited the best antibacterial property.

4. Discussions

The reason for chloride silver formation is that in a solution rich in chloride ions, such as SBF, silver "ions" not only belong to $Ag^{+}Cl$ but also to various ion pairs including

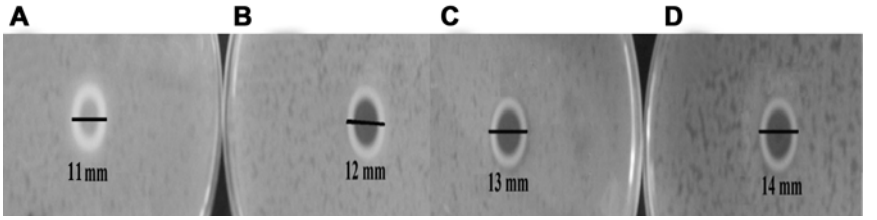

Fig. 5. Photograph of antibacterial 'halo' against *Escherichia coli* for (A) control, (B) 0.5% Ag-BG, (C) 1% Ag-BG, and (D) 2% Ag-BG.

Table 3. Width of antibacterial 'halo' and bactericidal ratio of samples with different amounts of silver

Analysis method	Ag_2O (mol%)			
	0	0.5	1	2
Width of antibacterial 'halo' (w/d)	0.05 ± 0.01	0.1 ± 0.1	0.15 ± 0.02	0.2 ± 0.1
Bactericidal ratio	100	100	100	100

$AgCl^{2-}$, $AgCl_3^{2-}$, $AgCl_4^{3-}$. However, it is obvious that only the ionic couple Ag^+Cl^- could lead to precipitation of silver chloride (AgCl(s)). In this connection, chloride ion acts as a buffer agent towards Ag^+, guaranteeing its fairly constant concentration in solution over the experimental conditions [37,38]. In this study, conventional SBF (c-SBF) was prepared according to the Kokubo's specification. As shown in Table 2, all constituents of plasma and SBF have identical concentrations except for HCO_3^-, which is less concentrated in SBF by a factor of approximately 6.4. In 2003, Oyane *et al*. attempted to correct this difference [29] by preparing a revised SBF (r-SBF) in which the concentrations of Cl^- and HCO_3^- ions were decreased and increased respectively to the levels of human blood plasma. However, calcium carbonate had a strong tendency to precipitate from this SBF, as it was supersaturated with respect to not only apatite, but also calcite. Calcite can have an effect on the procedure of apatite formation [29]. In 2004, Takadama *et al.* proposed a newly improved SBF (n-SBF) in which they decreased only the Cl^- ion concentration to the level of human blood plasma, leaving the HCO_3^- ion concentration equal to that of the conventional SBF (c-SBF) [30]. This improved SBF was compared with the c-SBF in its stability and the reproducibility of apatite formation on synthetic materials. Both SBFs were subjected to round robin testing in ten research institutes. As a result, the c-SBF was confirmed to not differ from n-SBF in stability and reproducibility [30]. Through this round robin testing, the method for preparing c-SBF was carefully checked and refined for easy preparation of SBF.

Higher solubility of silver-free bioactive glass in comparison with the silver containing samples was confirmed by its higher Si concentration in the SBF solution (according to the ICP measurement). It reflected the higher disruption rate of the control sample compared to silver glasses. Modifier elements caused the occurrence of non-bridging oxygen (NBO) and discontinuity in the vitreous network; but silver had an opposite effect in these samples [39]. In contrast, a higher concentration of modifiers in the glasses led to a higher degree of depolymerization in the structure and a higher concentration of the Si–O–NBO groups. These functional groups controlled the dissolution of silica through the formation of silanol in SBF. According to a report by Delben *et al.*, silver-containing bioactive glass samples seemed to increase bridging oxygen (BO) and phosphate bands. This fact can cause a solubility reduction of BG in SBF. In fact, the silver addition modifies the BG structure, increasing its density by reducing the amount of Si–O–NBO [39]. The reason for the decrease of Ca concentration in the solution was that when the apatite nuclei were formed, they grew spontaneously by consuming the calcium and phosphate ions in the surrounding fluid because the body fluid was highly supersaturated with respect to the apatite [40,41]. The slow release of the silver ion into the solution suggested that it was strongly chelated by the silicate network [26]. According to the ICP results, the release of silver ion for the 1 and 2% Ag-BG samples was lower than the 0.5% Ag-BG sample. The former was due to the silver chloride layer which inhibited a direct interaction between the glass surface and SBF solution, and the latter was attributed to the formation of a fully grown thicker apatite layer on the surfaces of the sample. It should be noted that the sliver chloride precipitation did form on each Ag-BG sample but the amount of formation of this layer was different for each sample. When the surface was covered by a thicker and denser layer of apatite or silver chloride, the dissolution rate slowed down or even stopped by inhibiting the exchange reaction between the bioactive glass and SBF. The competition between glass dissolution and apatite/AgCl precipitation rates is an important factor

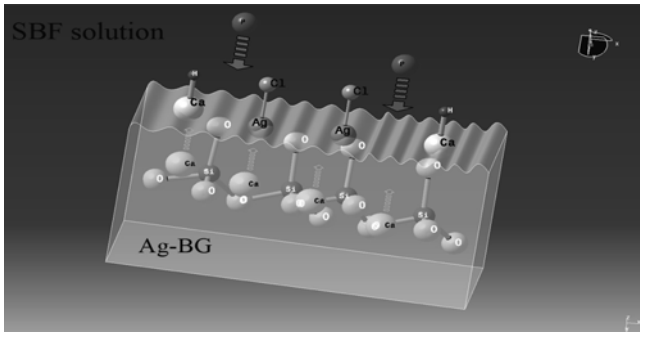

Fig. 6. The molecular interaction and nucleation mechanism at the Ag-BG interface.

which influences the release of silver ions in SBF.

As it can be seen in the FTIR spectra, the hydroxyapatite layer was detected for all samples after different times of immersion in SBF; it means that the presence of silver in the composition of bioactive glasses did not adversely affect the in vitro surface reactivity. Additionally, the release of Ag ions into SBF may reduce the minimum ion product of calcium and phosphate necessary for the precipitation of HCA [36]. As it can be observed, the sample containing 2% silver, kept for 14 days in SBF solution, exhibited a greater increase relative to the other samples. According to the ICP measurement and FTIR analysis, after the formation of the calcium phosphate layer, silver ions in the hydration layer might have bound phosphate ions and formed clusters of silver phosphate uniformly dispersed on apatite crystals [36]. These clusters might have acted as the nucleation sites for the precipitation of carbonated apatite. Based on the results, this mechanism was proven true for the 2% Ag-BG sample. This fact can confirm the above notes about the effect of silver in the formation of HCA. It is believed that the formation of biologically active carbonated apatite layer is a prerequisite for bioactive glasses and glass–ceramics to bond to the host tissue [42]. This mechanism is illustrated in Fig. 6.

Several suggestions have been made to elucidate the inhibitory effects of silver ions in bacteria. Microbiological and chemical experiments indicate that the antibacterial activity of silver is dependent on the cation (Ag^+), which binds strongly to electron donor groups on biological molecules containing sulfur, oxygen, phosphorus or nitrogen atoms. These atoms are present in organisms as thio, amino, carboxyl and phosphato groups. Silver ions are thought to interact with bacterial cell membrane proteins, inducing protein inactivation. Also, silver ions are known to affect the DNA molecules of bacteria and cause a loss in their ability to replicate [43]. As a result, bacterial death occurs due to the loss of function in the cell membrane or DNA of the bacteria such as transport, production and proliferation.

Table 4. The pH amounts of control and Ag-BG samples after different times of setting in the medium

Sample	pH		
	3 days	7 days	14 days
Ag free-BG (control)	7.65 ± 0.02	7.69 ± 0.01	8.1 ± 0.01
2% Ag-BG	7.9 ± 0.1	8.1 ± 0.2	8.9 ± 0.1

The antibacterial ring of the Ag-BG and Ag-free bioactive glass samples indicated that the halo width of silver containing samples was higher than the control. Table 4 provided evidence that high pH was responsible for the antibacterial activity. High pH solutions have previously been shown to have some antibacterial activity [44]. Dentifrices of high pH have also been shown to be bactericidal [45]. The antibacterial action of the glass was attributed to the high pH, ionic concentration produced when 1.7 g of powdered glass was suspended per milliliter of bacterial culture [46].

5. Conclusion

In this study, silver substituted bioactive glasses were prepared by the sol-gel method. It can be concluded from the results that after immersion of the Ag-BG samples in the SBF solution, silver chloride formed on the surface. Surface morphology of samples showed that apatite crystals with flake-like structure were formed on 2% Ag-BG, however, this kind of morphology was not observed in the other samples. Antibacterial properties of the silver containing bioactive glass indicated that the bactericidal ratio was better than the silver free bioactive glass against gram negative bacteria. In particular, the 2% Ag-BG glass sample showed a suitable antibacterial property. In fact, addition of silver into the BG structure induced formation of hydroxyapatite crystals with different morphological features and thus different surface reactivity. These findings suggest different bone bonding ability and biological responses which call for further *in vivo* assessments.

Acknowledgement

The authors gratefully acknowledge Iran National Science Foundation (INSF) for financial support of this work.

References

1. Moura, J., L. N. Teixeira, C. Ravagnani, O. Peitl, E. D. Zanotto,

and M. M. Beloti (2007) In vitro osteogenesis on a highly bioactive glassceramic (Biosilicate). *J. Biomed. Mater. Res. A* 82: 545-557.
2. Saravanapavan, P., J. R. Jones, S. Verrier, R. Beilby, V. J. Shirtliff, and L. L. Hench (2004) Binary CaO-SiO_2 gel-glasses for biomedical applications. *Biomed. Mater. Eng.* 14: 467-486.
3. Saravanapavan, P., J. R. Jones, R. S. Pryce, and L. L. Hench (2003) Bioactivity of gel-glass powders in the CaO-SiO2 system: A comparison with ternary (CaO-P2O5-SiO2) and quaternary glasses (SiO_2-CaO-P_2O_5-Na_2O). *J. Biomed. Mater. Res. A* 66: 110-119.
4. Oki, A., B. Parveen, S. Hossain, S. Adeniji, and H. Donahue (2004) Preparation and *in vitro* bioactivity of zinc containing sol-gel-derived bioglass materials. *J. Biomed. Mater. Res A* 69: 216-221.
5. Saboori, A., M. Sheikhi, F. Moztarzadeh, M. Rabiee, S. Hesaraki, and M. Tahriri (2009) Sol–gel preparation, characterisation and *in vitro* bioactivity of Mg containing bioactive glass. *Adv. Appl. Ceram.* 108: 155-161.
6. Balamurugan, A., A. H. Rebelo, A. F. Lemos, J. H. Rocha, J. M. Ventura, and J. M. Ferreira (2008) Suitability evaluation of sol-gel derived Si-substituted hydroxyapatite for dental and maxillofacial applications through *in vitro* osteoblasts response. *Dent. Mater.* 24: 1374-1380.
7. Balamurugan, A., G. Balossier, S. Kannan, J. Michel, A. H. Rebelo, and J. M. Ferreira (2007) Development and *in vitro* characterization of sol-gel derived CaO-P_2O_5-SiO_2-ZnO bioglass. *Acta Biomater.* 3: 255-262.
8. Buehler, J., P. Chappuis, J. L. Saffar, Y. Tsouderos, and A. Vignery A (2001) Strontium ranelate inhibits bone resorption while maintaining bone formation in alveolar bone in monkeys (Macaca fascicularis). *Bone* 29: 176-179.
9. Hott, M., P. Deloffre, Y. Tsouderos, and P. J. Marie (2003) S12911-2 reduces bone loss induced by short-term immobilization in rats. *Bone* 33: 115-123.
10. Meunier, P. J., C. Roux, E. Seeman, S. Ortolani, J. E. Badurski, T. D. Spector, and J. Cannata (2004) The effects of strontium ranelate on the risk of vertebral fracture in women with postmenopausal osteoporosis. *N Engl. J. Med.* 350: 459-468.
11. Seeman, E., J. P. Devogelaer, R. Lorenc, T. Spector, K. Brixen, A. Balogh, G. Stucki, and J. Y. Reginster (2008) Strontium ranelate reduces the risk of vertebral fractures in patients with osteopenia. *J. Bone Miner. Res.* 23: 433-438.
12. Panzavolta, S., P. Torricelli, L. Sturba, B. Bracci, R. Giardino, and A. Bigi (2008) Setting properties and *in vitro* bioactivity of strontium-enriched gelatin-calcium phosphate bone cements. *J. Biomed. Mater. Res. A* 84: 965-972.
13. Pietak, A. M., J. W. Reid, M. J. Stott, and M. Sayer (2007) Silicon substitution in the calcium phosphate bioceramics. *Biomaterials* 28: 4023-4032.
14. Phan, P. V., M. Grzanna, J. Chu, A. Polotsky, A. El-Ghannam, D. V. Heerden, D. S. Hungerford, and C. G. Frondoza (2003) The effect of silica-containing calcium-phosphate particles on human osteoblasts *in vitro*. *J. Biomed. Mater. Res. A* 67: 1001-1008.
15. Balamurugan, A., G. Balossier, J. Michel, S. Kannan, H. Benhayoune, A. H. Rebelo, and J. M. Ferreira (2007) Sol gel derived SiO_2-CaO-MgO-P_2O_5 bioglass system-preparation and in vitro characterization. *J. Biomed. Mater. Res. B (Appl. Biomater.)* 83: 546-553.
16. Jansen, B., M. Rinck, P. Wolbring, A. Strohmeier, and T. Jahnns (1994) *In vitro* evaluation of the antimicrobial efficacy and biocompatibility of a silver-coated central venous catheter. *J. Biomater. Appl.* 9: 55-70.
17. Kim, T. N., Q. L. Feng, J. O. Kim, J. Wu, H. Wang, G. C. Chen, and F. Z. Cui (1998) Antimicrobial effects of metal ions (Ag^+, Cu^{2+}, Zn^{2+}) in hydroxyapatite. *J. Mater. Sci. Mater. Med.* 9: 129-134.
18. Hoppe, A., N. S. Güldal, and A. R. Boccaccini (2011) A review of the biological response to ionic dissolution products from bioactive glasses and glass-ceramics. *Biomaterials* 32: 2757-2774.
19. Bellantone, M., H. D. Williams, and L. L. Hench (2002) Broad-spectrum bactericidal activity of Ag_2O-doped bioactive glass. *Antimocrob. Agents Chemother.* 46: 1940-1945.
20. Jones, J. R., L. M. Ehrenfried, P. Saravanapavan, and L. L. Hench (2006) Controlling ion release from bioactive glass foam scaffolds with antibacterial properties. *J. Mater. Sci. Mater. Med.* 17: 989-996.
21. Blaker, J. J., S. N. Nazhat, and A. R. Boccaccini (2004) Development and characterisation of silver doped bioactive glass coated sutures for tissue engineering and wound healing applications. *Biomaterials* 25: 1319-1329.
22. Durucan, C. and B. Akkopru (2010) Effect of calcination on microstructure and antibacterial activity of silver-containing silica coatings. *J. Biomed. Mater. Res. B. Appl. Biomater.* 93: 448-458.
23. Kawashita, M., S. Tsuneyama, F. Miyaji, T. Kokubo, H. Kozuka, and K. Yamamoto (2000) An antibacterial coating based on a polymer/sol-gel hybrid matrix loaded with silver nanoparticles. *Biomaterials* 21: 393-398.
24. Kawashita, M., S. Toda, H. M. Kim, T. Kokubo, and N. Masuda (2003) Preparation of antibacterial silver-doped silica glass microspheres. *J. Biomed. Mater. Res.* 66: 266-274.
25. Liu, H., Q. Chen, L. Song, R. Ye, J. Lu, and H. Li (2008) Ag-doped antibacterial porous materials with slow release of silver ions. *J. Non-Cryst. Solids* 354: 1314-1317.
26. Balamurugan, A., G. Balossier, D. Laurent-Maquin, S. Pina, A. H. S. Rebelo, J. Faure, and J. M. F. Ferreira (2008) An *in vitro* biological and anti-bacterial study on a sol–gel derived silver-incorporated bioglass system. *Dent. Mater.* 24: 1343-1351.
27. Raucci, M. G., K. Adesanya, L. D. Silvio, M. L. Catauro, and L. Ambrosio (2010) The biocompatibility of silver-containing Na_2O.CaO.2SiO_2 glass prepared by sol-gel method: *In vitro* studies. *J. Biomed. Mater. Res. B: Appl. Biomater*. 92: 102-110.
28. Kokubo, T., H. Kushitani, S. Sakka, T. Kitsugi, and T. Yamamuro (1990) Solutions able to reproduce *in vivo* surface-structure changes in bioactive glass-ceramic A-W. *J. Biomed. Mater. Res.* 24: 721-34.
29. Oyane, A., H. M. Kim, T. Furuya, T. Kokubo, T. Miyazaki, and T. Nakamura (2003) Preparation and assessment of revised simulated body fluid. *J. Biomed. Mater. Res.* 65: 188-195.
30. Takadama, H., M. Hashimoto, M. Mizuno, and T. Kokubo (2004) Round-robin test of SBF for *in vitro* measurement of apatite-forming ability of synthetic materials. *Phos. Res. Bull.* 17: 119-125.
31. Bell, R. J. and P. Dean (1970) Atomic vibrations in vitreous silica. *Discuss Faraday Soc.* 50: 55-61.
32. Gaskell, P. H. (1970) Vibrational spectra of simple silicate glasses. *Discuss Faraday Soc*. 50: 82-93.
33. LeGeros, R. F., G. Bone, and R. LeGeros (1978) Type of H_2O in human enamel and in precipitated apatites. *Calcif. Tissue Res.* 26: 111-118.
34. Li, P., A. E. Clark, and L. L. Hench (1992) Apatite formation induced by silica gel in a simulated body fluid. *J. Am. Ceram. Soc.* 75: 2094-2097.
35. Pereira, M. M., A. E. Clark, and L. L. Hench (1994) Calcium phosphate formation on sol-gel-derived bioactive glasses *in vitro*. *J. Biomed. Mater. Res.* 28:693-698.
36. Shirkhanzadeh, M. and M. Azadegan (1998) Formation of carbonate apatite on calcium phosphate coatings containing silver ions. *J. Mater. Sci.* 9: 385-391.
37. Daniele, P. G., C. D. Stefano, E. Prenesti, and S. Sammartano (1994) Weak complex formation in aqueous solution. In: Council

Scientific Information *(ed.). Current Topics in Solution Chemistry* 1: 95-106.
38. Chem, X., R. M. Izatt, and J. L. Oscarson (1994) Protons and metal ions in aqueous solutions at high temperatures. *Chem. Rev.* 94: 467-517.
39. Delben, J. R. J., O. M. Pimentel, M. B. Coelho, P. D. Candelorio, and L. N. Furini (2009) Synthesis and thermal properties of nanoparticles of bioactive glasses containing silver. *J. Therm. Anal. Calorim.* 97: 433-436.
40. Xue, W., J. L. Moore, H. L. Hosick, S. Bose, A. Bandyopadhyay, W. W. Lu, K. M. Cheung, and K. D. Luk (2006) Osteoprecursor cell response to strontium-containing hydroxyapatite ceramics. *J. Biomed. Mater. Res. A* 79: 804-814.
41. Kishi, Y., H. Shimojima, S. Ohsio, H. Saitoh, and K. Uematsu (1997) Microstructure design of HIPed TiO_2 ceramics for improved corrosion resistance *J. Mater. Sci. Lett.* 16: 1342-1344.
42. Annaz, B., K. A. Hing, M. Kayser, T. Buckland, and L. Di Silvio (2004) Porosity variation in hydroxyapatite and osteoblast morphology: A scanning electron microscopy study. *J. Microsc.* 21: 100-110.
43. Feng, Q. L., J. Wu, G. Q. Chen, F. Z. Cui, T. N. Kim, and J. O. Kim (2000) A mechanistic study of the antibacterial effect of silver ions on *Escherichia coli* and Staphylococcus aureus. *J. Biomed. Mat. Res.* 52: 662-668.
44. Barbosa, S. V., S. W. Spangberg, and D. Almedia (1994) Low surface tension calcium hydroxide solution is an elective antiseptic. *J. Int. Endodon.* 27: 6-10.
45. Drake, D. R., K. Vargas, A. Cardenzana, and R. Srikantha (1995) Enhanced bactericidal activity of arm and hammer dental Care. *Am. J. Dent.* 8: 308-3112.
46. Bellantone, M., N. J. Coleman, and L. L. Hench (2000) Bacteriostatic action of a novel four-component bioactive glass *J. Biomed. Mater. Res.* 51: 484-490.